

Universality and Shannon entropy of codon usage

L. Frappat^{ae}, C. Minichini^b, A. Sciarrino^{bd}, P. Sorba^c

^a *Laboratoire d'Annecy-le-Vieux de Physique Théorique LAPTH
CNRS, UMR 5108 associée à l'Université de Savoie
BP 110, F-74941 Annecy-le-Vieux Cedex, France*

^b *Dipartimento di Scienze Fisiche, Università di Napoli "Federico II"
^d I.N.F.N., Sezione di Napoli
Complesso Universitario di Monte S. Angelo
Via Cintia, I-80126 Naples, Italy*

^c *CERN, Theory Division, CH-1211 Geneva 23, Switzerland*

^e *Member of Institut Universitaire de France*

Abstract

The distribution functions of the codon usage probabilities, computed over all the available GenBank data, for 40 eukaryotic biological species and 5 chloroplasts, do not follow a Zipf law, but are best fitted by the sum of a constant, an exponential and a linear function in the rank of usage. For mitochondriae the analysis is not conclusive. A quantum-mechanics-inspired model is proposed to describe the observed behaviour. These functions are characterized by parameters that strongly depend on the total *GC* content of the *coding regions* of biological species. It is predicted that the codon usage is the same in all exonic genes with the same *GC* content. The Shannon entropy for codons, also strongly depending on the exonic *GC* content, is computed.

PACS number: 87.10.+e, 02.10.-v

1 Introduction

In the recent past, some interest has been shown in applying methods of statistical linguistics and information theory for the analysis of DNA sequences, in particular in investigating whether the frequency distribution of nucleotides or sequences of nucleotides follows Zipf's law [1], and using the Shannon entropy to identify the redundancy or the bias of a nucleotides sequence. Let us recall that, at the end of the forties, Zipf remarked that, in natural languages and in many other domains, the distribution function follows an inverse power law, which can be described, denoting by rank $n = 1$ the most used *word*, by $n = 2$ the next one and so on, and with $a > 0$, by

$$f_n = \frac{f_1}{n^a}. \quad (1)$$

In 1992, it was shown [2] that the distribution of the nucleotides in DNA follows a Zipf law of the type given by eq. (1). However, the opinions on this statement are divided, see [3]. Soon after [4, 5], it was shown that noncoding sequences of DNA are more similar to natural languages than the coding ones, and the Shannon entropy has been used to quantify the *redundancy* of word. This work also raised a debate in the literature [6]. Also, Zipf's law seems well adapted to represent the abundance of expressed genes, with an exponent $a \approx 1$, as can be seen in the recent work of ref. [7]. The origin of Zipf's law is thought to arise from stochastic processes [8], especially when they can be modelled as random walks in log scale [9]; for further analysis, see [10]. However, an analysis of the rank distribution for codons, performed in many genes for several biological species, led the authors of [12] to fit experimental data with an exponential function. In particular, by considering separately different coding DNA sequences, they studied the relation between the parameter in the exponential, the frequency of the rank one and the length of the sequence for different genes. From this very short overview, it follows that the determination of the kind of law the codon rank distribution follows is extremely interesting, in investigations of the nature of the evolutionary process, which has acted upon the codon distribution, i.e. the eventual presence of a bias.

In the last few years, the number of available data for coding sequences has considerably increased, but apparently no analysis using the whole set of data has been performed. The aim of this paper is to perform such a study. As the result of our investigation, we will point out that the rank of codon usage probabilities follows a universal law, the frequency function of the rank- n codon showing up as a sum of an exponential part and a linear part. A quantum-mechanics-inspired model is proposed, which provides for the form of the observed law and gives the correct sign in the different terms. Such a universal behaviour suggests the presence of general biases, one of which is identified with the total *exonic GC* content. Indeed, the values of the parameters appearing in the fitting expression are plotted versus the total percentage of exonic *GC* content of the biological species and are reasonably well fitted by a parabola. Finally, from the obtained expression, we derive the theoretical prediction that the usage probability for *rank-ordered* codons is the same in any genic region having the same exonic *GC* content for any biological species.

We compute the Shannon entropy [13] for amino-acids and find that its behaviour in function of the exonic *GC* content is also a parabola, whose apex is around the value 0.50 of the *GC* content.

2 Codon usage probabilities distribution

Let us define the usage probability for the codon XZN ($X, Z, N \in \{A, C, G, U\}$) as

$$P(XZN) = \lim_{n_{tot} \rightarrow \infty} \frac{n_{XZN}}{N_{tot}}, \quad (2)$$

where n_{XZN} is the number of times the codon XZN has been used in the analysed biosynthesis process for a given biological species and N_{tot} is the total number of codons used in all considered processes. It follows that our analysis and predictions hold for biological species with sufficiently large statistics of codons. For each biological species, codons are ordered following the decreasing order of the values of their usage probabilities, i.e. codon number 1 corresponds to the highest value, codon number 2 is the next highest, and so on. We denote by $f(n)$ the probability $P(XZN)$ of finding XZN is in the n -th position. Of course the same codon occupies in general two different positions in the rank distribution function for two different species. We plot $f(n)$ versus the rank and we determine that the best fit to the data can be reached by the sum of an exponential function, a linear function in the rank and a constant, i.e.

$$f(n) = \alpha e^{-\eta n} - \beta n + \gamma, \quad (3)$$

where $0.0187 \leq \alpha \leq 0.0570$, $0.050 \leq \eta \leq 0.136$, $0.82 \cdot 10^{-4} \leq \beta \leq 3.63 \cdot 10^{-4}$, $\gamma = 0,016$ are constant depending on the biological species. These four constants have to satisfy the normalization condition

$$\sum_n f(n) = 1. \quad (4)$$

In table 1 we list the 40 biological species (6 vertebrates, 4 plants, 3 invertebrates, 2 fungi and 25 bacteriae) – with a number of codons ranging between 800 000 and 20 000 000 in decreasing order (data from GenBank release 129.0 [17]), whose codon usage has been fitted, specifying for each biological species the value of the parameters, computed by a best-fit procedure and the corresponding χ^2 . Here and in the following, the χ^2 coefficient is defined by

$$\chi^2 = \sum_i \frac{(y_i - y(x_i))^2}{y(x_i)}, \quad (5)$$

where x_i are the experimental abscissae, y_i the experimental values and $y(x_i)$ the fitted ones. In some cases, $y(x_i)$ takes vanishing or negative values for a few points, hence the χ^2 is not reported. In figs. 1–4, we report the plot of $f(n)$ as a function of n for a few biological species (*Homo sapiens*, *Drosophila melanogaster*, *Arabidopsis thaliana*, and *Escherichia coli*). The plot has been cut to $n = 61$ to take into account the fact that in standard code there are three Stop codons (to end the biosynthesis process), whose function is very peculiar. For the same reason, the χ^2 has been computed by taking into account the 61 coding codons only. In table 6, we report the type of the twenty-first most used codons of the observed rank distribution $f(n)$. A similar study, for a sample of twenty vertebrates with a codon statistics larger than 100 000, reveals that, for almost all biological species, the four most used codons are *GAG*, *CUG*, *AAG* and *CAG*. All these codons have a *G* nucleotide in third position and three of them encode doublets. An analysis performed on the chloroplast codon usage for a sample of five plants gives the same result for the rank distribution $f(n)$, see table 2 and fig. 5 (*Chloroplast Arabidopsis thaliana*). We also report, in table 3, the values of the parameters and the χ^2 for a sample of nine mitochondriae with a codon statistics larger than

15 000. The fits for *Homo sapiens* and *Arabidopsis thaliana* are presented in figs. 6 and 7. We point out, however, that for mitochondriae the codon usage frequencies distribution for several species (e.g. *Arabidopsis thaliana* or *Drosophila melanogaster*) is ill fitted by eq. (3). It may be an indication that mitochondriae do not follow the universal law (3). Note that the mitochondrial codes have a few differences with the eukaryotic code and vary slightly between species, see e.g. [11]. In these cases, the χ^2 has been computed over the corresponding coding codons. The value of the constant γ is approximately equal to $1/61 = 0.0164$ or to $1/64 = 0.0156$, i.e. the value of the codon usage probability in the case of uniform and not biased codon distribution. Therefore the other two terms in eq. (3) can be viewed as the effect of the bias mechanism. The appearance of the linear term is more intriguing. Let us remark that in [12], where an exponential function is used to fit the rank of usage in genes (not the rank of usage probability), the linear term has not been observed, as its contribution becomes noticeable for approximately $n \geq 20$. Owing to the analysis of genes (with at most a few hundred codons), the fits in that paper end before this value of the rank. It is believed that the main causes of codon usage bias are the translational efficiency, the selection pressure and the spontaneous mutations. From the smallness of parameter β in (3), it is tempting to identify the latter as the consequence of mutation effect and the first term in (3) as the effect of selection pressure, i.e. the interaction with the environment.

Let us try to build up a simple model to explain the universal structure of eq. (3). In a physical quantum system, with discrete energy levels, the occupation number of the i -th energetic level is proportional to $\exp(-E_i/kT)$, where E_i is the energy of the level, T is identified with the temperature and k is the Boltzmann constant. Inspired by this analogy, let us assume that the rank of the probability distribution is a function of some kind of *energy*. In this case the codon usage probability is, for any codon, equal to $f(n) = \exp(-aE_n)$, where a is a positive constant. We assume that the system satisfies periodic conditions in the y and z directions, with a very small spacing in the z direction, so that the excited modes along this direction can be neglected, and that the interaction with the environment can be modelled as the switching on of a constant uniform *magnetic field* in the direction of the z axis. As a consequence, the Landau levels appear, the *energetic levels* now being in natural units

$$E_n - E_0 = \omega(n + 1/2), \quad (6)$$

where ω is the so-called cyclotron frequency. The wave function is

$$\psi(x, y, z) = \Phi_n(x - lx_0) e^{ik_y y} e^{ik_z z}, \quad (7)$$

where

$$k_y = \frac{2\pi l}{L_y}, \quad k_z = \frac{2\pi}{L_z}, \quad l \in \mathbf{Z}, l \neq 0, \quad (8)$$

and $\Phi_n(x - lx_0)$ is the wave function of the n -th energy level of a one-dimensional harmonic oscillator shifted by lx_0 ($x_0 = 2\pi/qBL_y$). There is a degeneracy due to the arbitrariness of k_y . A quantum charged physical system in an excited state spontaneously falls down to a lower state, the equilibrium configuration being the system in the fundamental state. In the case of codons, the equilibrium condition is the configuration where they occupy different “energy” levels, the situation being the analogue of a quantum system in the presence of an external pumping-back source. In order to model this situation in a simple way, we assume that the equilibrium probability distribution is a function $f(n) - f(n)_{B=0} = F(E_n, \gamma_n)$, where γ_n is the “spontaneous emission coefficient” of the n -th

level, which is taken to be very small because of the assumed equilibrium condition. We can make a first-order development in γ_n :

$$f(n) - f(n)_{B=0} = F(E_n, \gamma_n = 0) + \frac{dF}{d\gamma_n}, \quad (9)$$

where $dF/d\gamma_n$ is negative, the occupation probability decreasing with the increasing emission. We compute γ_n in the standard dipole approximation [14] between the n -th and the k -th levels ($k < n$). In the case of our model, we get

$$\gamma_n \propto n \delta_{k,n-1}. \quad (10)$$

So, replacing $F(E_n, \gamma_n = 0)$ by the Maxwell–Boltzmann expression, we obtain eq. (3). The values of the parameters depend on the biological species, as the selection pressure (in the model, the value of the *charge* and of the *magnetic field*) is different for different biological species. Even if our simple model is able to explain the universal behaviour and the right sign of the linear term, one should rather consider it as a toy model. However, the fact that one can build a simple mathematical scenario, able to reproduce the observed distribution, provides us with an indication of the existence of some strong physico-chemical constraints that add to the random effects.

Since it is well known that the *GC* content plays a strong role in the evolutionary process, we expect the parameters to depend on the total *GC* content of the genes region (here the total exonic *GC* content), which is indeed correlated with the evolution of the system (see [15] and references therein). We have investigated this dependence and report, in table 4, the fits of α and β to the total exonic *GC* content Y_{GC} of the biological species. One finds that the values of α and β are well fitted by polynomial functions (with $0 \leq Y_{GC} \leq 100$ in percentage):

$$\alpha = 0.21145 - 0.00776 Y_{GC} + 7.92 \cdot 10^{-5} Y_{GC}^2, \quad \chi^2 = 0.0262, \quad (11)$$

$$10^2 \beta = 0.10096 - 0.00345 Y_{GC} + 3.50 \cdot 10^{-5} Y_{GC}^2, \quad \chi^2 = 0.0170. \quad (12)$$

The two parameters α and β appear to be correlated. Indeed the plot representing β as a function of α is satisfactorily fitted by a regression line (see fig. 4):

$$10^2 \beta = 0.00851 + 0.375 \alpha, \quad \chi^2 = 0.0218. \quad (13)$$

The value of the η parameter is largely uncorrelated with the total exonic *GC* content. Let us recall that, however, η is a function of α and β due to the normalization condition of eq. (4). Indeed we have (assuming $e^{-65\eta} \approx 0$)¹

$$1 = \frac{\alpha e^{-\eta}}{1 - e^{-\eta}} + 2080\beta + 64\gamma. \quad (14)$$

Using the fits for α and β , we can write the probability distribution function for any biological species, whose total *GC* content in per cent in the exonic regions is Y_{GC} , as

$$f(n) = (\alpha_0 + \alpha_1 Y_{GC} + \alpha_2 Y_{GC}^2) e^{-\eta n} - n(\beta_0 + \beta_1 Y_{GC} + \beta_2 Y_{GC}^2) + \gamma, \quad (15)$$

where η is obtained by solving eq. (14). Of course we are not able to predict which codon occupies the n -th rank. Finally, let us remark that the total exonic *GC* content Y_{GC} has to satisfy the consistency condition

$$Y_{GC} = \frac{1}{3} \sum_{i \in I} d_i f(i), \quad (16)$$

where the sum is over the set I of integers to which the 56 codons containing *G* and/or *C* nucleotides belong and d_i is the multiplicity of these nucleotides inside the i -th codon.

¹Note that the result is almost unchanged if the data are normalized on the 61 coding codons.

3 Amino-acids rank distribution

It is natural to wonder if some kind of universality is also present in the rank distribution of amino-acids. From the available data for codon usage, we can immediately compute (using the eukaryotic code) the frequency of appearance of any amino-acid $F(n)$ ($1 \leq n \leq 20$) in the whole set of coding sequences. The calculated values as a function of the rank are satisfactorily fitted by a straight line,

$$F(n) = F_0 - Bn . \quad (17)$$

The parameters F_0 , B and the corresponding χ^2 for the fits are reported in table 7. A better fit can be obtained in general by using a third-degree polynomial; however, the range of the four parameters for this fit is larger than the range of the 2-parameter fit. For a few biological species, we give below the parameters for the two fits, see also the figures of table 9. The plots of the linear fits for few biological species are given in table 8. Note that the 21st point is just the contribution of the Stop codons, which of course has not been taken into account for the fits. One can remark that the most frequent amino-acid is always above the line. This can be easily understood in the light of eq. (3). Indeed, the most frequent amino-acids get, in general, a contribution of the exponential term of (3) with a low value of n .

Species	linear/cubic fits	χ^2
Homo sapiens	lin. $f = 0.087 - 0.0036n$	0.0072
	cub. $f = 0.099 - 0.0088n + 57 \cdot 10^{-5}n^2 - 1.7 \cdot 10^{-5}n^3$	0.0055
Arabidopsis thaliana	lin. $f = 0.088 - 0.0036n$	0.0068
	cub. $f = 0.099 - 0.0090n + 62 \cdot 10^{-5}n^2 - 1.95 \cdot 10^{-5}n^3$	0.0049
Drosophila melanogaster	lin. $f = 0.087 - 0.0036n$	0.0125
	cub. $f = 0.097 - 0.0096n + 76 \cdot 10^{-5}n^2 - 2.5 \cdot 10^{-5}n^3$	0.0042
Escherichia coli	lin. $f = 0.090 - 0.0039n$	0.0115
	cub. $f = 0.112 - 0.0136n + 105 \cdot 10^{-5}n^2 - 3.1 \cdot 10^{-5}n^3$	0.0067

Of course, the frequency of an amino-acid is given by the sum of the frequencies of its encoding codons given by (3). If the ranks of the encoding codons were completely random, we do not expect that their sum should take equally spaced values, as is the case in a regression line. Therefore, we can infer, for the biological species whose amino-acids frequency is very well fitted by a line, the existence of some functional constraints on the codon usage.

We report in table 10 the distribution of the amino-acids for the different biological species.

However, the behaviour predicted by eq. (3) fits the experimental data very well, while the shape of the distribution of amino-acids seems more sensible to the biological species. In fact, one can remark on many plots of the amino-acid distributions (see e.g. table 8), the existence of one or two plateaux, for which we do not have any explanation yet.

4 Consequences of probability distribution

We now derive a few consequences of eq. (3). In the following, we denote by y the *local* exonic *GC* content (i.e. for coding sequences of genes) for a given biological species. Let us assume that the exonic *GC* content of a biological species is essentially comprised in the interval $y_1 - y_0 = \Delta$ (e.g.

for *Homo sapiens* $y_0 = 35\%$ and $y_1 = 70\%$). We can write

$$f(n) = \frac{1}{\Delta} \int_{y_0}^{y_1} f(y, n) dy . \quad (18)$$

Since the l.h.s. of the above equation has the form given by eq. (3) for any n and for any biological species, if we do not want to invoke some “fine tuning” in the integrand function $f(y, n)$, we have to assume that

$$f(y, n) = a(y)e^{-\eta n} - b(y)n + \gamma \quad (19)$$

with the condition

$$\alpha = \frac{1}{\Delta} \int_{y_0}^{y_1} a(y) dy , \quad \beta = \frac{1}{\Delta} \int_{y_0}^{y_1} b(y) dy . \quad (20)$$

As a consequence, we predict that the codon usage probability is the same for any codon in any exonic genic region with the same GC content. The form of the $a(y)$ and $b(y)$ functions is yet undetermined. For *Homo sapiens*, we remark that the total exonic GC content Y_{GC} is, in a very good approximation, equal to the mean value of the interval $[y_0, y_1]$. Therefore, inserting (18) and (19) into (16), we derive that the functions $a(y)$ and $b(y)$ have to be *linear* functions of y . This theoretical derivation is in accordance with the conclusions of Zeeberg [16] obtained by an analysis for 7357 genes. On a quantitative level, using the numerical linear fits of Zeeberg, we find a very good agreement with our calculations. Note that this result is not in contradiction with eq. (15), since the previous analysis is valid for the fixed value of the exonic GC content for *Homo sapiens*. For bacteriae, the range of variation Δ of the local exonic GC content is very small. Therefore we expect the functions $a(y)$ and $b(y)$ to have the same shape as the functions α and β given in eqs. (11) and (12). Hence the functions α and β depend on the biological species.

We compute the Shannon entropy, given by

$$S = - \sum_n f(n) \log_2 f(n) \quad (21)$$

for the codons of a biological species and plot it versus the total exonic GC content; see figure in table 4. The Shannon entropy is rather well fitted by a parabola:

$$S = 2.2186 + 0.144 Y_{GC} - 0.00146 Y_{GC}^2 , \quad \chi^2 = 0.0315 . \quad (22)$$

Note that the parabola has its apex for $y \approx 0.50$, which is expected for the behaviour of the Shannon entropy for two variables (here GC and its complementary AU).

The same behaviour have been put in evidence by analogous computations made by Zeeberg [16] for *Homo sapiens*. So it seems that the entropy in the gene coding sequences and the total exonic region entropy in function of the exonic GC content show the same pattern.

In conclusion, the distribution of the experimental codon probabilities for a large total exonic region of several biological species has been very well fitted by the law of eq. (3). The spectrum of the distribution is universal, but the codon, which occupies a fixed level, depends on the biological species. Indeed, a more detailed analysis shows that, for close biological species, e.g. vertebrates, a fixed codon occupies almost the same position in $f(n)$, while for distant biological species the codons occupy very different positions in the rank distribution. We have also derived that the codon frequency for any genic region is, for fixed biological species and fixed GC content, the same. Entropy

analysis has shown that the behaviour observed in the genes with different GC content for the same biological species is very similar to the one shown by the total exonic region with different GC content for the different biological species.

Acknowledgements: The authors would like to thank A. Arneodo for fruitful discussions. A.S. is indebted to the Université de Savoie for financial support and LAPTH for its kind hospitality.

References

- [1] G.K. Zipf, *Human behaviour and the Principle of Least Effort* (Addison-Wesley Press, Cambridge, MA, 1949).
- [2] R.F. Voss, Phys. Rev. Lett. **68** (1992) 3805; W. Li and K. Kaneko, Europhys. Lett. **17** (1992) 655; C.-K. Peng, S.V. Buldyrev, S. Havlin, H.E. Stanley and A.L. Goldberger, Nature **356** (1992) 168.
- [3] S. Nee, Nature **357** (1992) 450; S. Karlin and V. Brendel, Science **259** (1993) 677; D. Larhammar and C.A. Chatzidimitriou-Dreissman, Nucl. Acid. Res. **21** (1993) 450.
- [4] R.N. Mantegna, S.V. Buldyrev, A.L. Goldberger, S. Havlin, C.-K. Peng, M. Simons and H.E. Stanley, Phys. Rev. Lett. **73** (1994) 3169.
- [5] A. Czirok, R.N. Mantegna, S. Havlin and H.E. Stanley, Phys. Rev. E **52** (1995) 446.
- [6] R. Israeloff, M. Kagalenko and K. Chan, Phys. Rev. Lett. **76** (1996) 1976; S. Bonhoeffer, A.V.M. Herz, M.C. Boerlijst, S. Nee, M.A. Nowak and R.M. May, Phys. Rev. Lett. **76** (1996) 1997; R.F. Voss, Phys. Rev. Lett. **76** (1996) 1978; R.N. Mantegna, S.V. Buldyrev, A.L. Goldberger, S. Havlin, C.-K. Peng, M. Simons and H.E. Stanley, Phys. Rev. Lett. **76** (1996) 1979.
- [7] C. Furusawa and K. Kaneko, *Zipf's Law in Gene Expression*, physics/0209103.
- [8] A. Czirok, H.E. Stanley and T. Vicsek, Phys. Rev E **53** (1996) 6371.
- [9] K. Kawamura and N. Hatano, *Universality of Zipf law*, cond-mat/0203455.
- [10] Ph. Bronlet and A. Ausloos, *Generalized (m,k) Zipf law for fractional Brownian motion-like series with or without effect of an additional linear trend*, cond-mat/0209306.
- [11] L. Frappat, A. Sciarrino and P. Sorba, J. Biol. Phys. **17** (2001) 1.
- [12] A. Som, S. Chattapadhyay, J. Chakrabarti and D. Bandyopadhyay, Phys. Rev. E **63** (2001) 051908.
- [13] C.E. Shannon, Bell System Tech. J. **27** (1948) 623.
- [14] J.J. Sakurai, *Advanced Quantum Mechanics* (Addison Wesley, Redwood City, CA, 1967) (Xth edition, chap. 2).
- [15] R.D. Knight, S.J. Freeland, L.F. Landweber, Genome Biol. **2** (2001) 1, (<http://genomebiology.com/2001/2/4/research/0010>).

- [16] B. Zeeberg, *Genome Research* **12** (2002) 944,
(<http://www.genome.org/cgi/doi/10.1101/gr.213402>).
- [17] Y. Nakamura, T. Gojobori and T. Ikemura, *Nucl. Acids Res.* **28** (2000) 292,
<http://www.kazusa.or.jp/codon/>.

Table 1: Values of the best-fit parameters, eq. (3), for the sample of biological species. Types: vrt = vertebrates (6), inv = invertebrates (3), pln = plants (4), fng = fungi (2), bct = bacteriae (25).

Type	Species	<i>GC</i> content in %	α	η	$10^4 \beta$	χ^2
vrt	Homo sapiens	52.58	0.0214	0.073	1.65	0.0126
pln	Arabidopsis thaliana	44.55	0.0185	0.056	1.68	0.0051
inv	Drosophila melanogaster	54.03	0.0247	0.081	1.67	0.0089
inv	Caenorhabditis elegans	42.79	0.0216	0.064	1.79	0.0063
vrt	Mus musculus	52.38	0.0208	0.071	1.57	0.0112
fng	Saccharomyces cerevisiae	39.69	0.0246	0.069	1.91	0.0127
bct	Escherichia coli	50.52	0.0233	0.065	1.91	0.0112
vrt	Rattus norvegicus	52.87	0.0222	0.073	1.63	0.0083
pln	Oryza sativa japonica	55.84	0.0179	0.073	1.63	0.0211
fng	Schizosaccharomyces pombe	39.80	0.0255	0.068	1.98	0.0036
bct	Bacillus subtilis	44.32	0.0259	0.084	1.71	0.0241
bct	Pseudomonas aeruginosa	65.70	0.0538	0.107	2.76	0.0191
bct	Mesorhizobium loti	63.05	0.0416	0.093	2.44	0.0093
bct	Streptomyces coelicolor A3	72.41	0.0567	0.098	3.14	0.0456
bct	Sinorhizobium meliloti	62.71	0.0359	0.076	2.54	0.0067
bct	Nostoc sp. PCC 7120	42.36	0.0288	0.098	1.63	0.0140
pln	Oryza sativa	54.63	0.0173	0.062	1.59	0.0135
bct	Agrobacterium tumefaciens str. C58	59.74	0.0308	0.067	2.43	0.0100
bct	Ralstonia solanacearum	67.57	0.0543	0.105	2.87	0.0149
bct	Yersinia pestis	48.97	0.0179	0.040	2.17	0.0066
bct	Methanosarcina acetivorans str. C24	45.17	0.0228	0.068	1.81	0.0214
bct	Vibrio cholerae	47.35	0.0203	0.052	2.02	0.0100
bct	Escherichia coli K12	51.83	0.0250	0.065	2.05	0.0117
bct	Mycobacterium tuberculosis CDC1551	65.77	0.0401	0.094	2.35	0.0105
bct	Mycobacterium tuberculosis H37Rv	65.90	0.0414	0.097	2.29	0.0109
bct	Bacillus halodurans	44.32	0.0263	0.100	1.27	0.0233
bct	Clostridium acetobutylicum	31.59	0.0434	0.087	2.76	–
bct	Caulobacter crescentus CB15	67.68	0.0570	0.113	2.86	0.0087
vrt	Gallus gallus	52.11	0.0239	0.095	1.17	0.0129
bct	Synechocystis sp. PCC6803	48.56	0.0260	0.083	1.49	0.0140
bct	Sulfolobulus solfataricus	36.47	0.0290	0.066	2.26	0.0099
bct	Mycobacterium leprae	59.90	0.0252	0.071	1.80	0.0065
bct	Brucella melitensis	58.25	0.0294	0.067	2.25	0.0121
bct	Deinococcus radiodurans	67.24	0.0481	0.098	2.76	0.0113
vrt	Xenopus laevis	47.33	0.0193	0.084	0.92	0.0268
bct	Listeria monocytogenens	38.39	0.0437	0.136	1.64	0.0267
pln	Neurospora crassa	56.17	0.0241	0.086	1.31	0.0166
bct	Clostridium perfringens	29.47	0.0510	0.092	3.11	–
inv	Leishmania major	63.36	0.0294	0.069	2.21	0.0050
vrt	Bos taurus	53.05	0.0240	0.089	1.27	0.0126

Table 2: Values of the best-fit parameters, eq. (3), for the sample of chloroplasts.

Species	<i>GC</i> content in %	α	η	$10^4 \beta$	χ^2
<i>Arabidopsis thaliana</i>	38.37	0.0254	0.067	1.95	0.0030
<i>Chaetosphaeridium globosum</i>	30.29	0.0515	0.110	2.59	0.0174
<i>Chlorella vulgaris</i>	34.63	0.0513	0.114	2.04	0.0093
<i>Cyanidium caldarium</i>	33.31	0.0379	0.092	2.24	0.0103
<i>Guillardia theta</i>	33.20	0.0452	0.103	2.20	0.0089

Table 3: Values of the best-fit parameters, eq. (3), for the sample of mitochondriae.

Type	Species	<i>GC</i> content in %	α	η	$10^4 \beta$	χ^2
vert	<i>Homo sapiens</i>	44.99	0.0414	0.099	2.31	0.0207
pln	<i>Arabidopsis thaliana</i>	44.18	0.0136	0.049	1.39	0.0589
vert	<i>Mus musculus</i>	37.23	0.0455	0.104	2.44	0.0226
fng	<i>Saccharomyces cerevisiae</i>	24.17	0.0879	0.198	2.66	0.0611
inv	<i>Physarum polycephalum</i>	25.69	0.0624	0.128	2.70	0.0262
pln	<i>Pylaiella littoralis</i>	37.06	0.0336	0.108	1.72	0.0112
pln	<i>Neurospora crassa</i>	33.20	0.0388	0.101	2.14	0.0225
vert	<i>Bos taurus</i>	39.73	0.0422	0.106	2.25	0.0430
vert	<i>Sus scrofa</i>	40.52	0.0497	0.112	2.51	0.0372

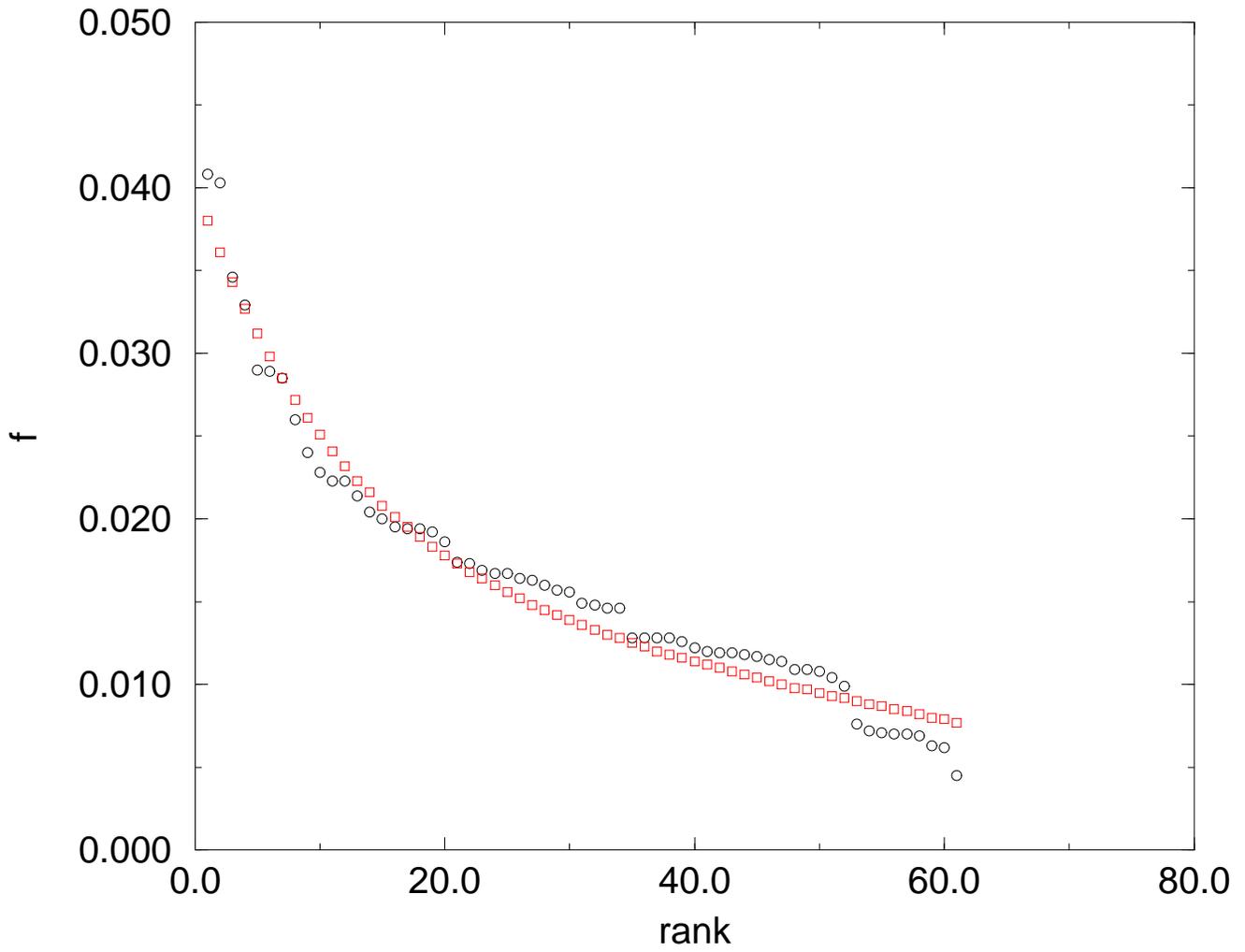


Figure 1: Rank distribution of the codon usage probabilities for *Homo sapiens*. Circles are experimental values, squares are fitted values.

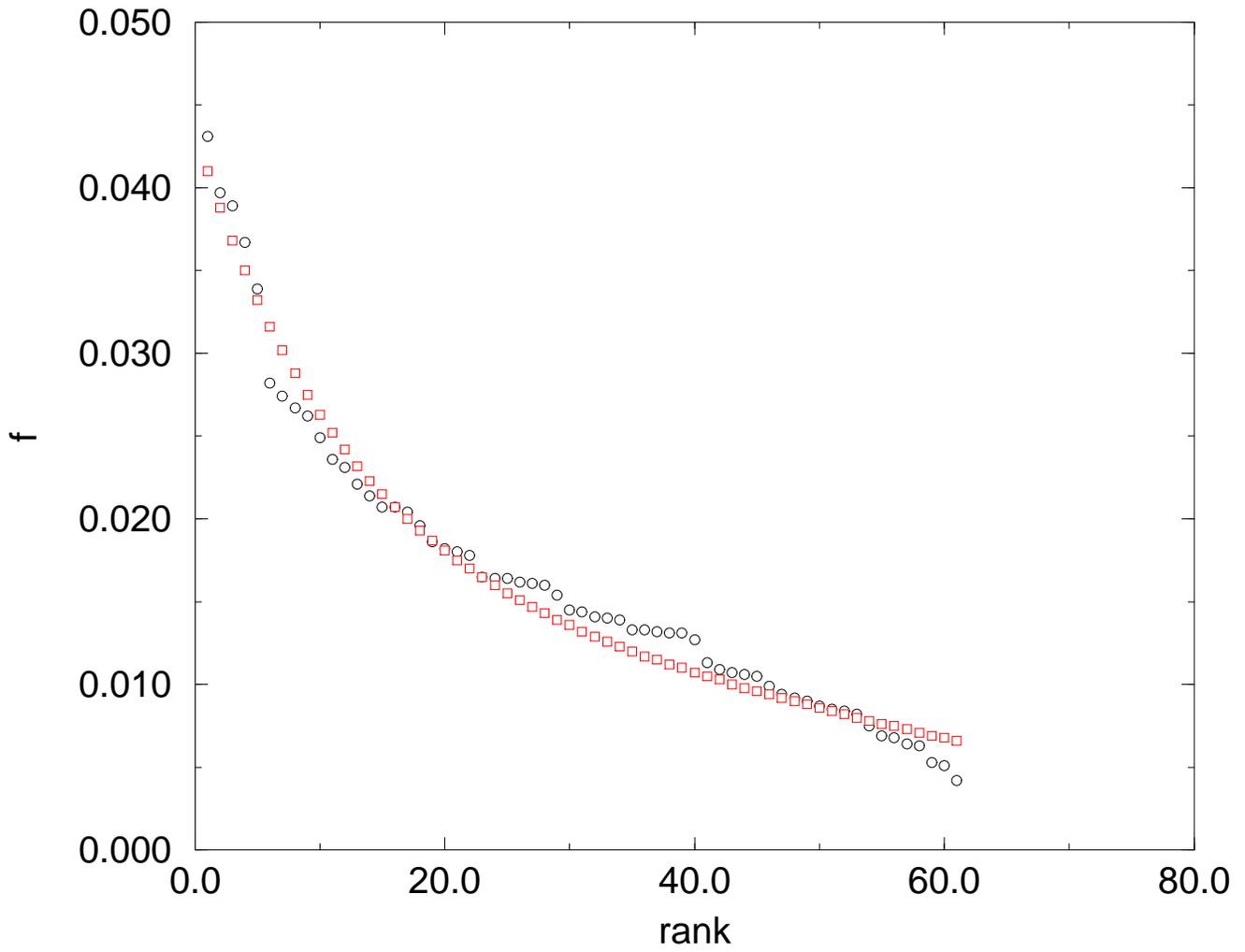


Figure 2: Rank distribution of the codon usage probabilities for *Drosophila melanogaster*. Circles are experimental values, squares are fitted values.

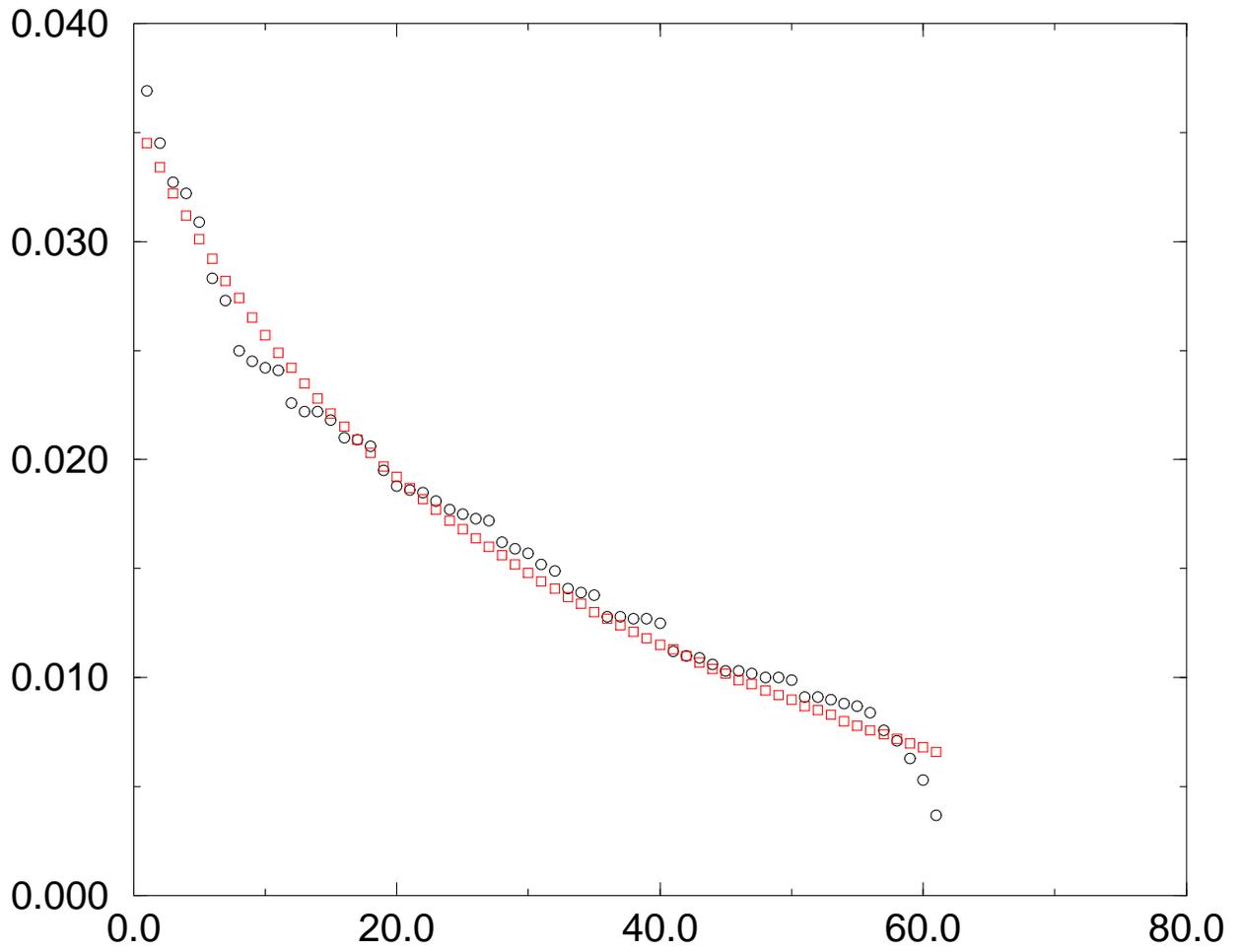


Figure 3: Rank distribution of the codon usage probabilities for *Arabidopsis thaliana*. Circles are experimental values, squares are fitted values.

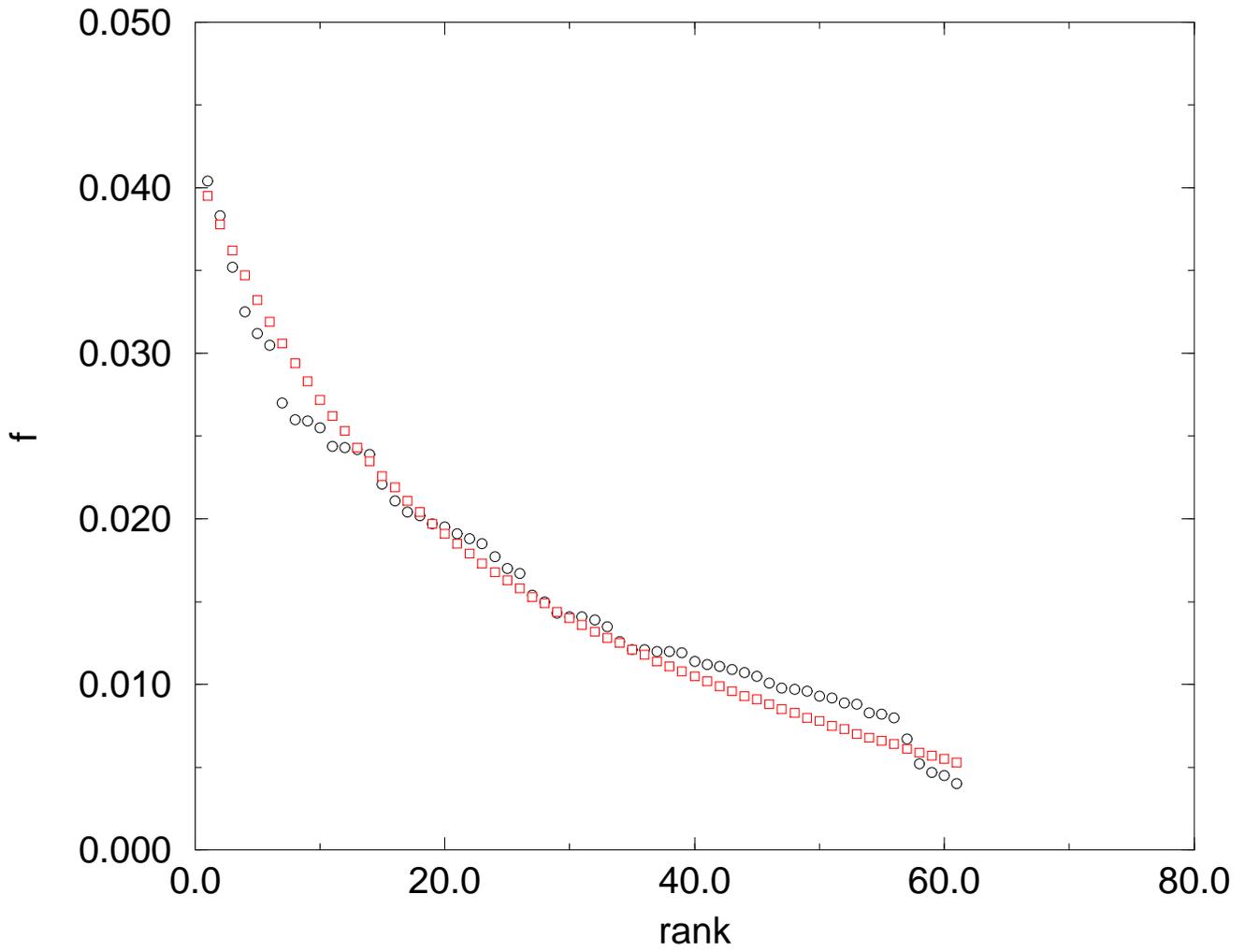


Figure 4: Rank distribution of the codon usage probabilities for *Escherichia coli*. Circles are experimental values, squares are fitted values.

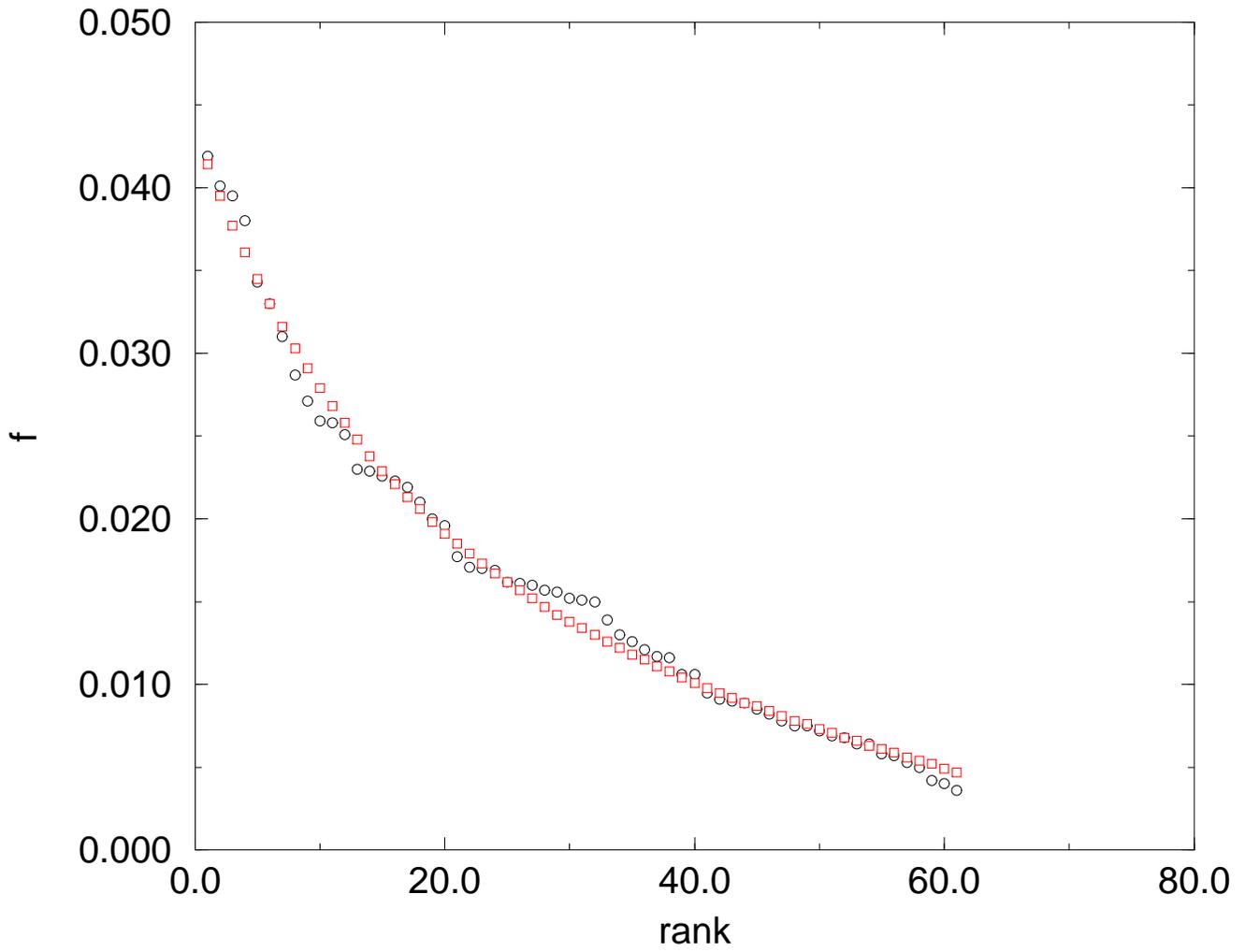


Figure 5: Rank distribution of the codon usage probabilities for *Chloroplast Arabidopsis thaliana*. Circles are experimental values, squares are fitted values.

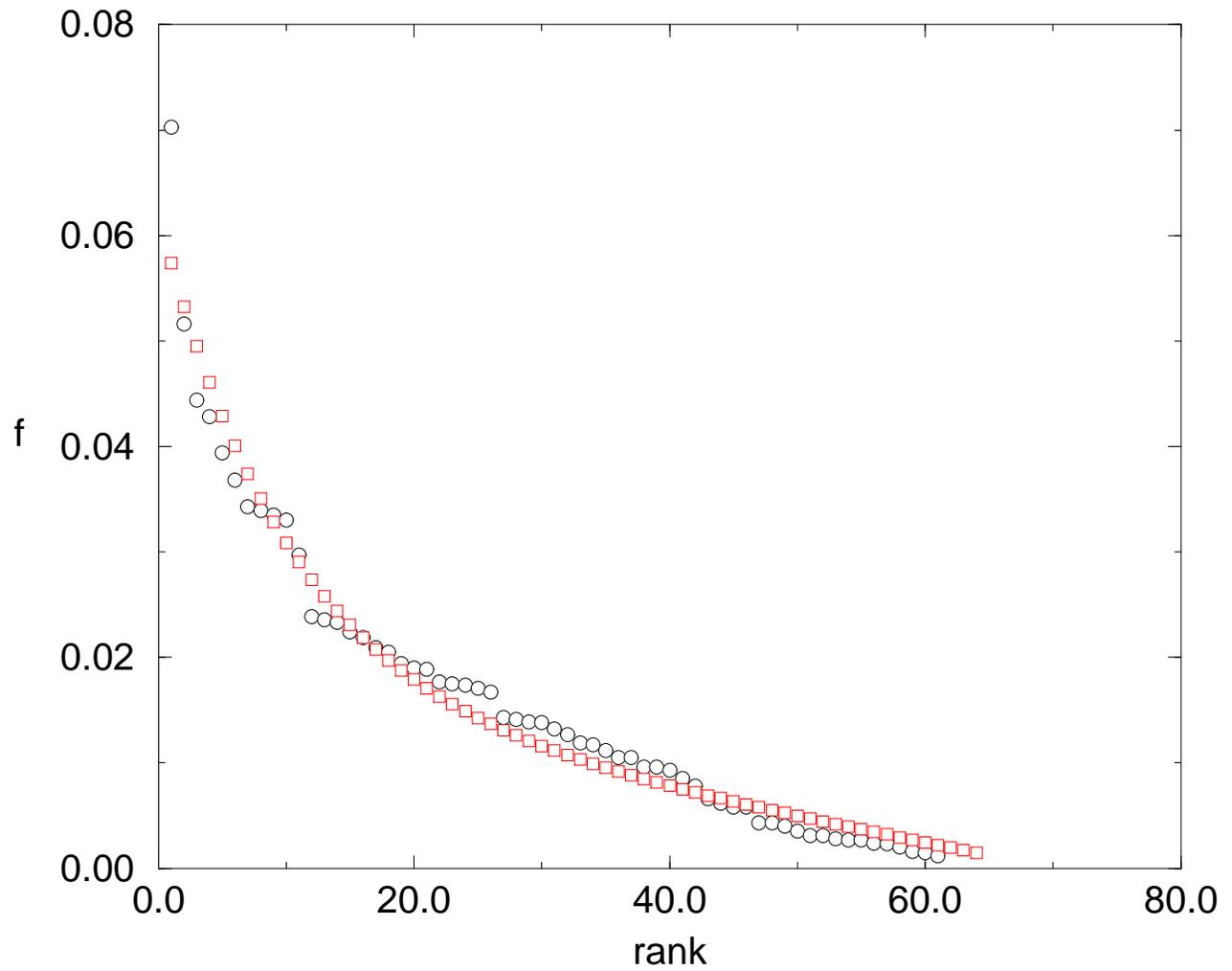


Figure 6: Rank distribution of the codon usage probabilities for *Mitochondrial Homo sapiens*. Circles are experimental values, squares are fitted values.

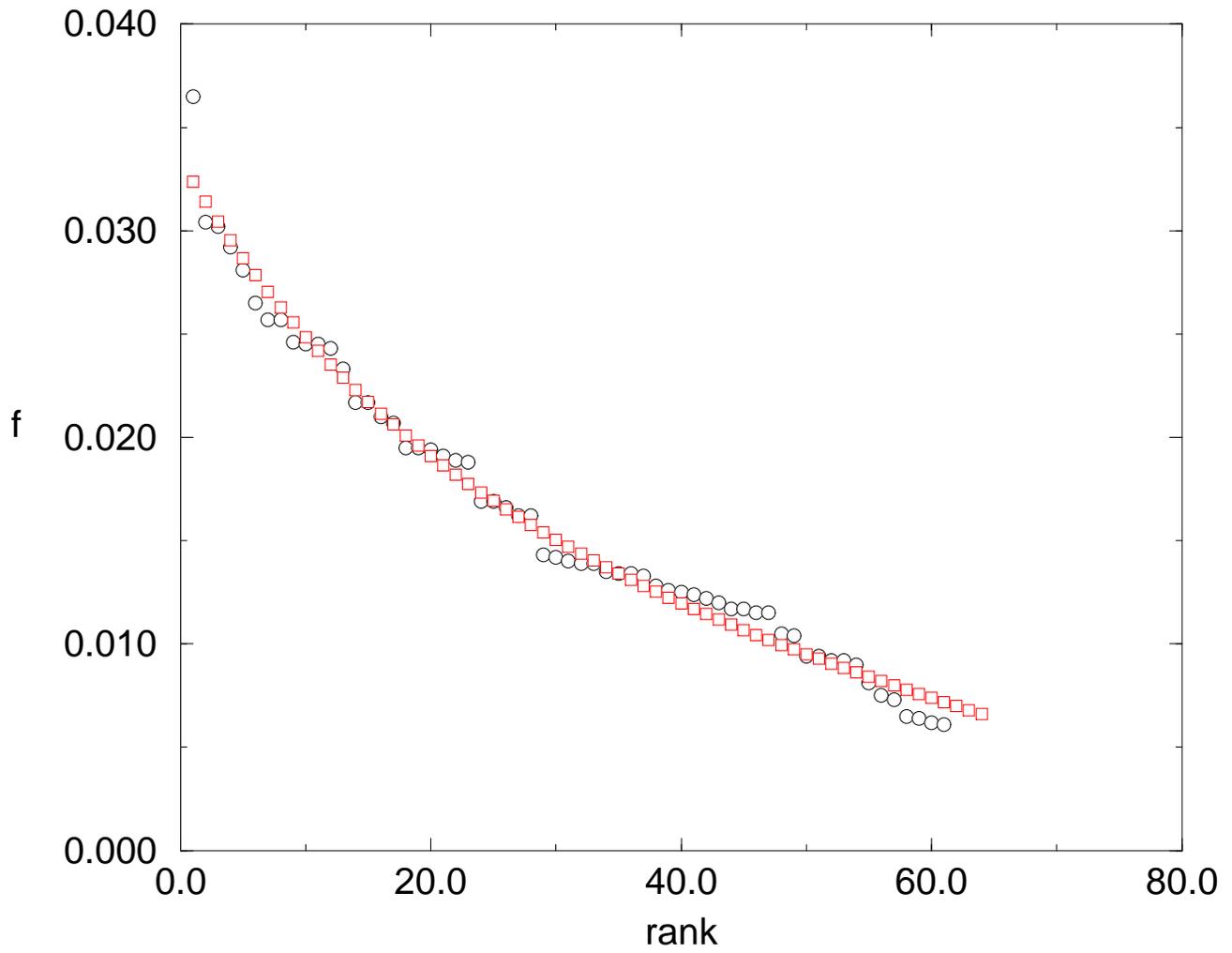
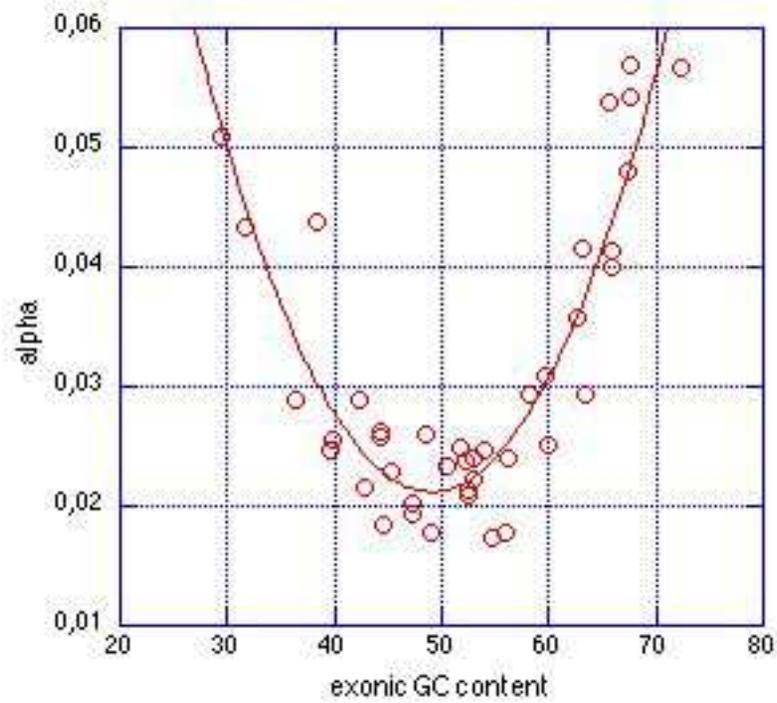
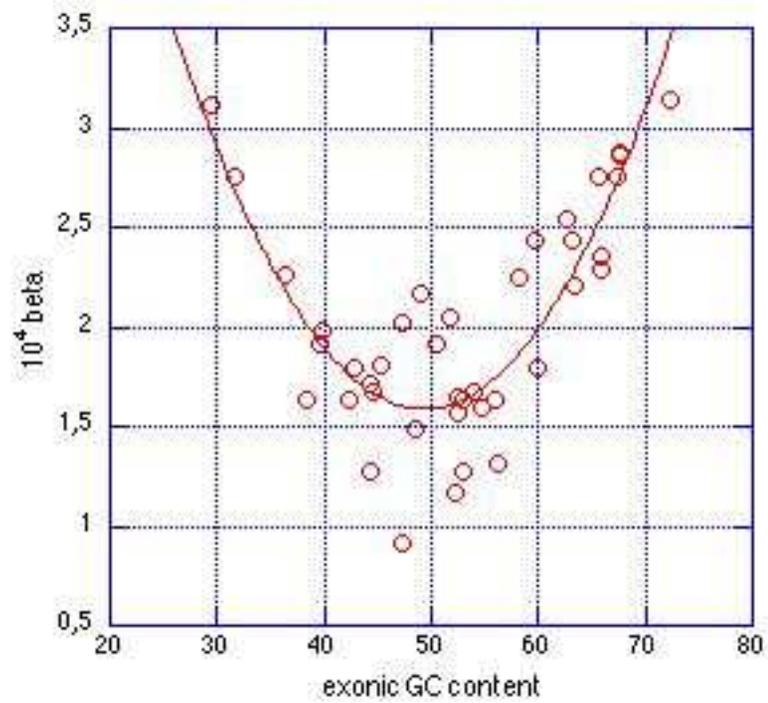


Figure 7: Rank distribution of the codon usage probabilities for *Mitochondrial Arabidopsis thaliana*. Circles are experimental values, squares are fitted values.

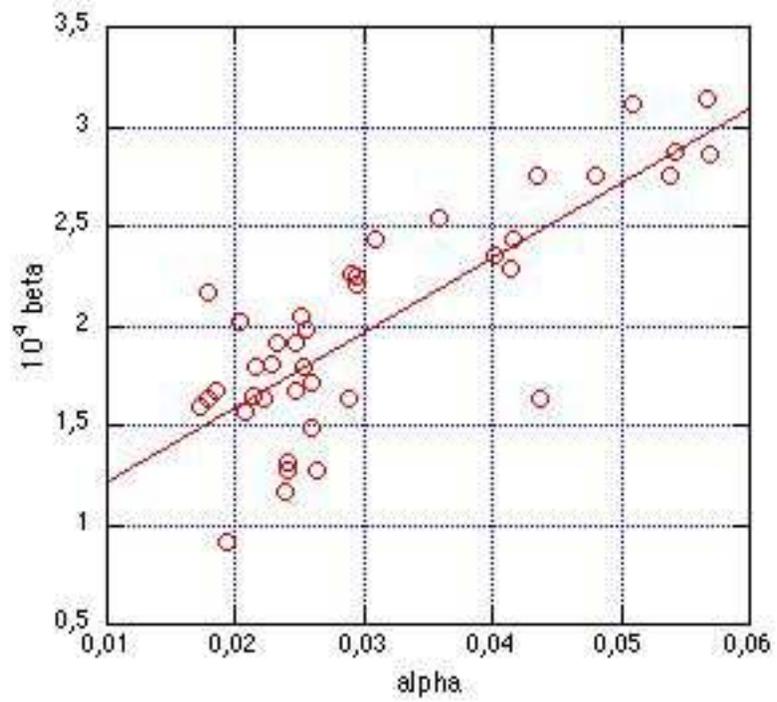


α vs. the exonic GC content

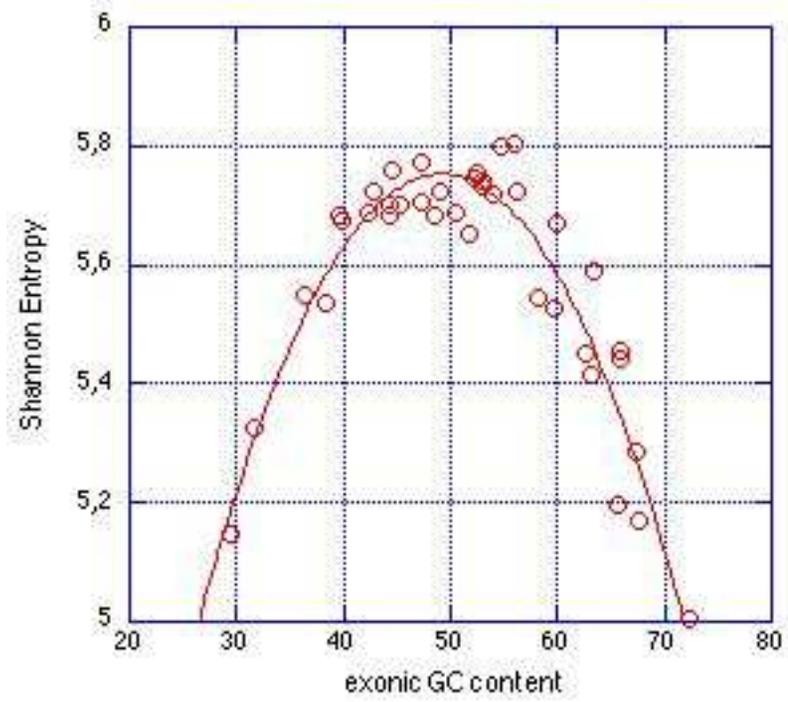


β vs. the exonic GC content

Table 4: Fits for the α and β parameters.



Fit for β as a function of α



Shannon entropy vs. the exonic *GC* content

Table 5: Fits for the α , β parameters and for the Shannon entropy.

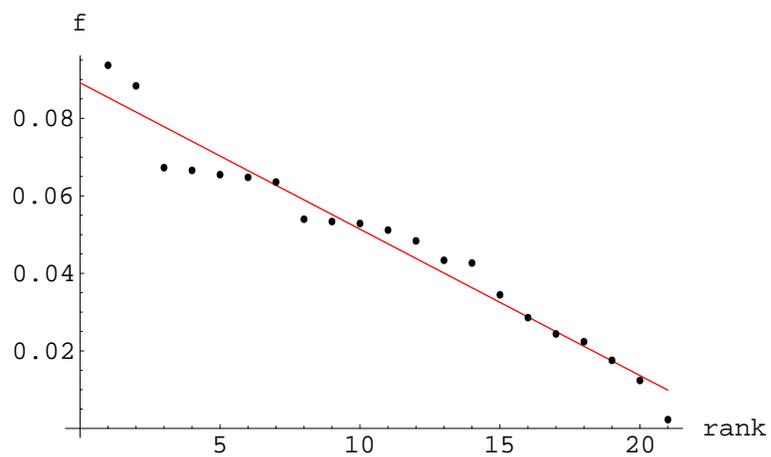
Table 6: Type of used codons of the observed rank distribution $f(n)$.

Rank	1	2	3	4	5	6	7	8	9	10	11	12	13	14	15	16	17	18	19	20
Homo sapiens	GAG	CUG	CAG	AAG	GAA	GUG	GCC	GAC	AAA	GGC	AUG	GAU	AUC	UUC	CCC	AAC	CUC	AGC	ACC	GCU
Mus musculus	CUG	GAG	AAG	CAG	GUG	GAC	GAA	GCC	AUC	AUG	GGC	UUC	GAU	AAA	AAC	CUC	GCU	AGC	ACC	CCC
Rattus norvegicus	CUG	GAG	AAG	CAG	GUG	GAC	GCC	GAA	AUC	UUC	AUG	AAC	GGC	CUC	GAU	AAA	ACC	AGC	GCU	CCC
Gallus gallus	GAG	CUG	AAG	CAG	GAA	GUG	AAA	GAC	GCC	GAU	AAC	AUC	AUG	GGC	AGC	UUC	GCU	CCC	UAC	ACC
Xenopus laevis	GAA	GAG	AAA	AAG	CAG	GAU	CUG	AUG	GAC	AAU	AAC	GGA	GUG	GCU	CCA	AUU	GCA	UUU	UCU	ACA
Bos taurus	CUG	GAG	AAG	CAG	GUG	GCC	GAC	GAA	AUC	GGC	UUC	AAC	AUG	AAA	ACC	GAU	CUC	CCC	UAC	AGC
Arabidopsis thaliana	GAU	GAA	AAG	GAG	AAA	GCU	GUU	UCU	AUG	CUU	GGA	AAU	GGU	UUU	AUU	UUG	AAC	UUC	CAA	AGA
Oryza sativa japonica	GAG	GCC	GGC	AAG	GAC	GCG	CUC	GUG	GAU	AUG	UUC	CUG	GAA	CAG	GUC	AUC	CCG	GCU	AAC	CGC
Oryza sativa	GAG	AAG	GCC	GGC	GAC	GAU	CUC	AUG	GUG	GCG	UUC	CAG	GAA	AUC	GCU	AAC	GUC	CUG	GCA	GGG
Neurospora crassa	GAG	AAG	GCC	GAC	GGC	AAC	CUC	AUC	CAG	GUC	ACC	GAU	CCC	UUC	AUG	GAA	GCU	UCC	GGU	UAC
Drosophila melanogaster	GAG	AAG	CUG	CAG	GCC	GUG	GAU	GGC	AAC	GAC	AUG	AUC	UUC	ACC	GAA	AAU	AGC	UCC	UAC	CGC
Caenorhabditis elegans	GAA	AAA	GAU	AUU	GGA	AAU	CAA	AUG	AAG	CCA	UUU	UUC	GAG	GUU	GCU	CUU	UCA	UUG	ACA	GCA
Leishmania major	GCG	GAG	GCC	CUG	GUG	GGC	GAC	CAG	CGC	AAG	CCG	AGC	CUC	ACG	AUG	AAC	UCG	CAC	GCA	UAC
Sacch. cerevisiae	GAA	AAA	GAU	AAU	AAG	AUU	CAA	UUG	UUA	UUU	AAC	GGU	UCU	GUU	AGA	GCU	AUG	GAC	ACU	GAG
Schizosacch. pombe	GAA	AAA	GAU	AUU	AAU	UUU	UCU	GCU	GUU	CAA	UUA	CUU	AAG	UUG	ACU	UAU	CCU	GGU	GAG	AUG
Escherichia coli	CUG	GAA	AAA	GAU	GCG	AUU	CAG	GGC	AUG	GGU	GUG	GCC	AUC	UUU	ACC	AAC	GCA	CCG	AAU	CGU
Bacillus subtilis	AAA	GAA	AUU	GAU	UUU	AUC	AUG	GGC	GAG	CUG	CUU	UAU	AAU	ACA	GGA	GCA	AAG	GCG	CAA	UUA
Pseudom. aeruginosa	CUG	GCC	GGC	CGC	GAC	GCG	AUC	GAG	CAG	GUG	UUC	ACC	CCG	GUC	CUC	AAG	AGC	GAA	AAC	AUG
Mesorhizobium loti	GGC	GCC	CUG	AUC	GCG	GUC	GAC	CGC	UUC	GAG	CCG	AAG	CUC	GUG	ACC	CAG	AUG	GAA	UCG	GAU
Streptom. coelicolor A3	GCC	GGC	CUG	GAC	GCG	GAG	GUC	ACC	CGC	CUC	GUG	CCG	CGG	AUC	UUC	CCC	CAG	CAC	UCC	AAG
Sinorhizobium meliloti	GGC	GCC	GCG	AUC	GUC	CUC	CUG	GAC	CGC	GAG	UUC	CCG	AAG	GAA	AUG	CAG	GUG	ACC	ACG	UCG
Nostoc sp. PCC 7120	GAA	AUU	CAA	UUA	AAA	GAU	AAU	UUU	GCU	GGU	GCA	UUG	GUU	ACU	UAU	GUA	ACA	AUC	GCC	AUG
Agrobact. tumefaciens	GCC	GGC	CUG	AUC	GCG	GAA	CGC	GUC	UUC	GAU	GAC	AAG	CUC	CCG	AUG	GUG	CAG	GAG	ACC	ACG
Ralstonia solanacearum	CUG	GCC	GGC	GCG	GCG	GUG	AUC	GAC	CCG	CAG	GAG	UUC	ACC	GUC	AAG	ACG	AUG	AAC	UCG	CUC
Yersinia pestis	CUG	GAU	GAA	AAA	AUU	GCC	AUG	GGU	CAG	AAU	GCG	GGC	CAA	AUC	UUG	GUG	UUU	ACC	UUA	GAG
Methanosarc. acetivorans	GAA	AAA	CUU	GAU	GGA	AUU	GCA	AUC	GAG	UUU	CUG	GAC	AUG	AAU	AAG	AAC	AUA	GUU	UAU	UUC
Vibrio cholerae	GAA	GAU	AAA	CAA	AUU	GCG	GUG	UUU	CUG	GGU	AUG	AUC	GAG	GGC	UUG	AAU	GCC	UUA	GCU	ACC
Escherichia coli K12	CUG	GAA	GCG	AAA	GAU	AUU	GGC	CAG	AUG	GUG	GCC	AUC	GGU	ACC	CCG	UUU	CGC	AAC	CGU	GCA
Mycobact. tuber. CDC1551	GCC	CUG	GGC	GCG	GAC	GUG	ACC	AUC	GUC	CCG	GAG	CGC	CGG	CAG	UUC	UCG	AAC	GGG	GGU	AUG
Mycobact. tuber. H37Rv	GCC	GGC	CUG	GCG	GAC	GUG	ACC	AUC	GUC	CCG	GAG	CGC	CGG	UUC	CAG	AAC	UCG	GGG	GGU	AUG
Bacillus halodurans	GAA	AUU	AAA	GAU	UUU	GAG	CAA	UUA	AUG	AUC	UAU	CUU	GGA	GUU	AAG	ACG	AAU	GCA	GUG	GCG
Clostridium acetobutylicum	AAA	AUA	AAU	GAA	GAU	UUU	UUA	AUU	UAU	GGA	AAG	GUU	GUA	CUU	GCA	AUG	AGA	GCU	ACA	GGU
Caulobacter crescentus CB15	GCC	CUG	GGC	GCG	GAC	CGC	AUC	GUC	GAG	ACC	AAG	UUC	GUG	CCG	CAG	AUG	UCG	AAC	CCC	CUC
Synechocystis sp. PCC 6803	GAA	AUU	GCC	CAA	GAU	UUG	AAA	UUU	GUG	ACC	UUA	CCC	AAU	GGC	CAG	CUG	GCU	GGU	AUG	GAC
Sulfolobus solfataricus	AUA	UUA	AAA	GAA	AAG	GAU	AUU	AAU	UAU	GAG	GUA	GUU	UUU	GGA	AGA	GCU	GGU	AUG	ACU	GCA
Mycobacterium leprae	GCC	CUG	GUG	GAC	GCG	GGC	AUC	GUC	ACC	GAG	CCG	UUG	GGU	CGC	CAG	GAU	GAA	GCU	UUC	CGG
Brucella melitensis	GGC	GCC	CUG	GAA	GCG	GCG	AUC	GAU	AAG	GUG	CCG	UUC	AUG	CAG	CUU	GAC	GUC	ACC	CUC	GAG
Deinococcus radiodurans	CUG	GCC	GGC	GUG	GCG	GAC	CGC	ACC	CAG	CUC	GAG	CCC	GAA	CCG	AGC	GUC	AUC	UUC	GGG	CGG
Listeria monocytogenes	AAA	GAA	AUU	GAU	UUA	AAU	UUU	CAA	GCA	GUU	AUG	ACA	GGU	UAU	GCU	GUA	CUU	GGA	AUC	CCA
Clostridium perfringens	AAA	GAA	UUA	AUA	AAU	GAU	GGA	UUU	GUU	UAU	AUU	GCU	AGA	AAG	GUA	AUG	ACU	UCA	GCA	ACA

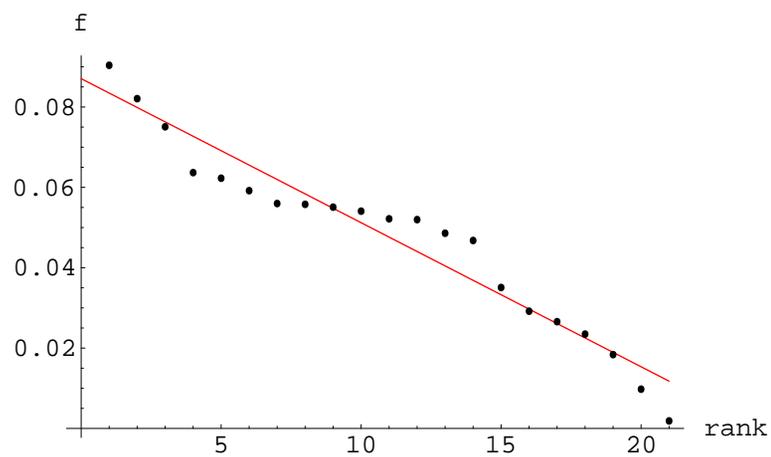
Table 7: Values of the best-fit parameters for the amino-acids.

Species	$10^3 B$	F_0	χ^2
Homo sapiens	3.8	0.089	0.0072
Arabidopsis thaliana	3.8	0.090	0.0068
Drosophila melanogaster	3.5	0.087	0.0125
Caenorhabditis elegans	3.3	0.084	0.0124
Mus musculus	3.7	0.088	0.0087
Saccharomyces cerevisiae	3.9	0.090	0.0121
Escherichia coli	4.0	0.091	0.0115
Rattus norvegicus	3.7	0.088	0.0084
Oryza sativa japonica	4.1	0.093	0.0057
Schizosaccharomyces pombe	3.8	0.089	0.0162
Bacillus subtilis	4.0	0.091	0.0104
Pseudomonas aeruginosa	4.9	0.101	0.0493
Mesorhizobium loti	4.7	0.100	0.0215
Streptomyces coelicolor A3	5.6	0.109	0.0624
Sinorhizobium meliloti	4.7	0.100	0.0188
Nostoc sp. PCC 7120	4.0	0.092	0.0174
Oryza sativa	3.9	0.091	0.0028
Agrobacterium tumefaciens str. C58	4.6	0.098	0.0144
Ralstonia solanacearum	4.7	0.101	0.0351
Yersinia pestis	4.0	0.092	0.0135
Methanosarcina acetivorans str. C2A	4.1	0.092	0.0063
Vibrio cholerae	3.9	0.091	0.0148
Escherichia coli K12	4.0	0.091	0.0154
Mycobacterium tuberculosis CDC1551	5.2	0.105	0.01121
Mycobacterium tuberculosis H37Rv	5.3	0.106	–
Bacillus halodurans	4.0	0.091	0.0100
Clostridium acetobutylicum	4.6	0.097	0.0076
Caulobacter crescentus CB15	5.1	0.104	0.0524
Gallus gallus	3.6	0.088	0.0040
Synechocystis sp. PCC 6803	4.1	0.093	0.0168
Sulfolobus solfataricus	4.4	0.096	0.0143
Mycobacterium leprae	4.9	0.101	0.0401
Brucella melitensis	4.5	0.097	0.0142
Deinococcus radiodurans	5.2	0.105	0.0679
Xenopus laevis	3.5	0.086	0.0084
Listeria monocytogenes	4.2	0.093	0.0088
Neurospora crassa	4.0	0.091	0.0042
Clostridium perfringens	4.6	0.098	0.0035
Leishmania major	4.7	0.099	0.0367
Bos taurus	3.6	0.087	0.0082

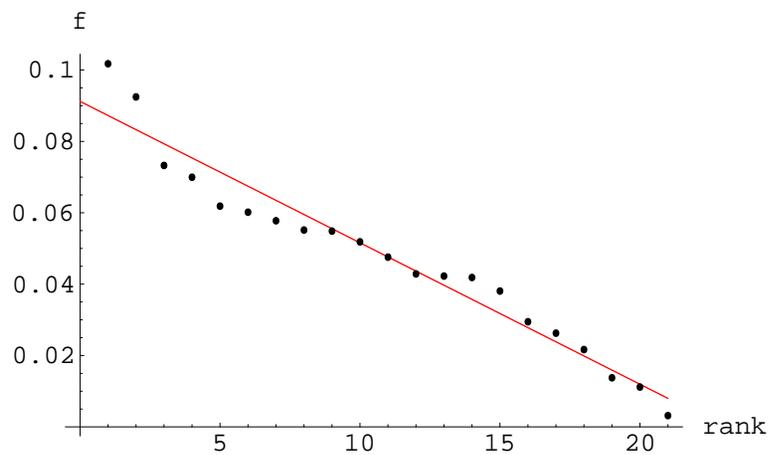
Table 8: Amino-acids rank distributions.



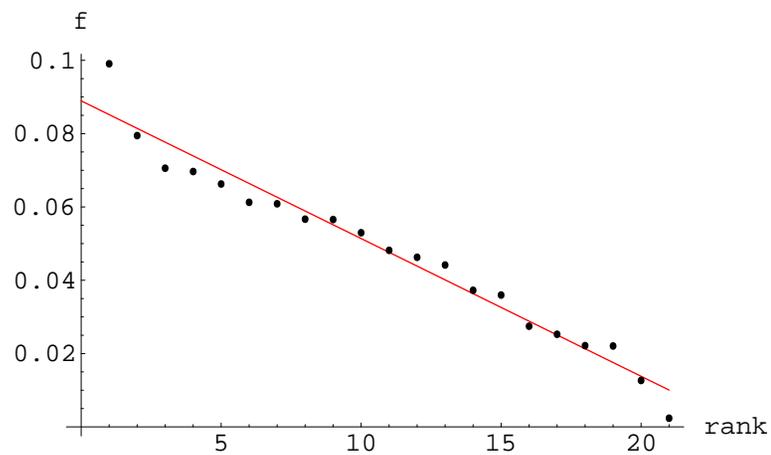
Arabidopsis thaliana



Drosophila melanogaster

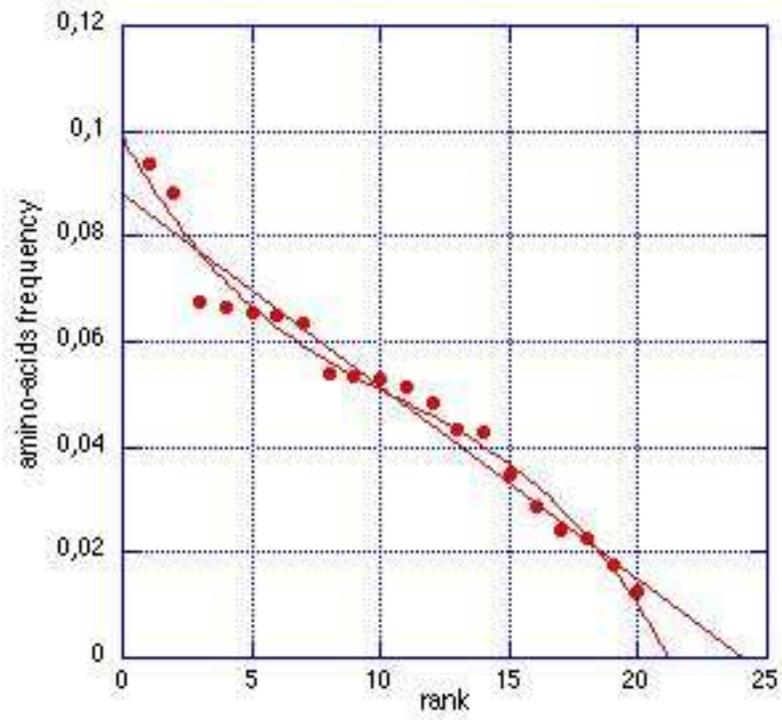


Escherichia coli

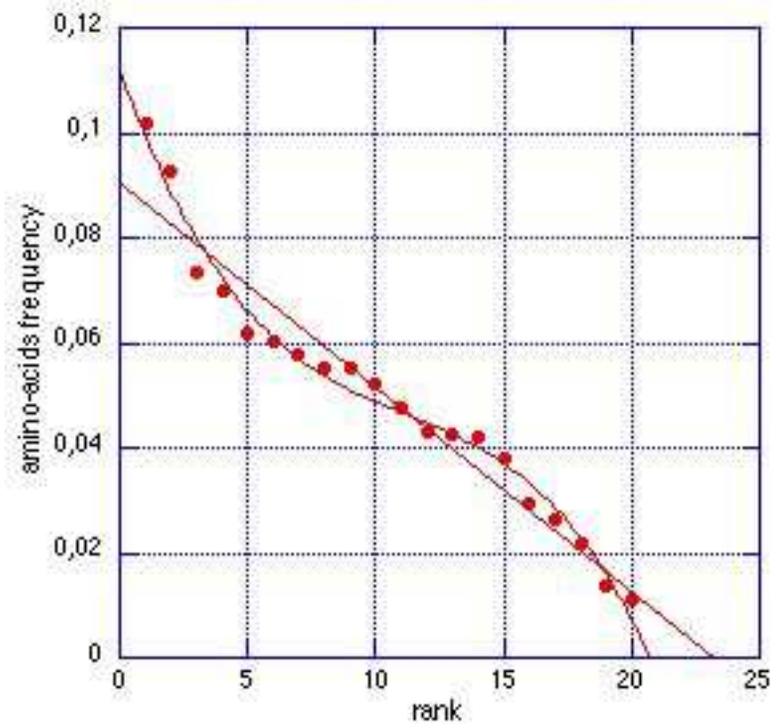


Homo sapiens

Table 9: Amino-acids rank distributions : linear vs. cubic fits.



Arabidopsis thaliana



Escherichia coli

Table 10: Type of used amino-acids of the observed rank distribution.

Rank	1	2	3	4	5	6	7	8	9	10	11	12	13	14	15	16	17	18	19	20
Homo sapiens	Leu	Ser	Ala	Glu	Gly	Val	Pro	Lys	Arg	Thr	Asp	Gln	Ile	Phe	Asn	Tyr	His	Met	Cys	Trp
Mus musculus	Leu	Ser	Ala	Gly	Glu	Val	Pro	Lys	Arg	Thr	Asp	Ile	Gln	Phe	Asn	Tyr	His	Cys	Met	Trp
Rattus norvegicus	Leu	Ser	Ala	Glu	Gly	Val	Pro	Lys	Thr	Arg	Asp	Ile	Gln	Phe	Asn	Tyr	His	Met	Cys	Trp
Gallus gallus	Leu	Ser	Glu	Ala	Gly	Lys	Val	Pro	Thr	Arg	Asp	Ile	Gln	Asn	Phe	Tyr	His	Met	Cys	Trp
Xenopus laevis	Leu	Ser	Glu	Lys	Ala	Gly	Val	Pro	Thr	Asp	Arg	Ile	Gln	Asn	Phe	Tyr	Met	His	Cys	Trp
Bos taurus	Leu	Ser	Ala	Gly	Glu	Val	Lys	Pro	Thr	Arg	Asp	Ile	Gln	Phe	Asn	Tyr	Cys	His	Met	Trp
Arabidopsis thaliana	Leu	Ser	Val	Glu	Gly	Ala	Lys	Asp	Arg	Ile	Thr	Pro	Asn	Phe	Gln	Tyr	Met	His	Cys	Trp
Oryza sativa japonica	Ala	Leu	Gly	Ser	Arg	Val	Glu	Pro	Asp	Thr	Lys	Ile	Phe	Gln	Asn	His	Tyr	Met	Cys	Trp
Oryza sativa	Ala	Leu	Gly	Ser	Arg	Val	Glu	Pro	Asp	Lys	Thr	Ile	Phe	Gln	Asn	Tyr	His	Met	Cys	Trp
Neurospora crassa	Ala	Leu	Ser	Gly	Glu	Pro	Arg	Thr	Val	Asp	Lys	Ile	Gln	Asn	Phe	Tyr	His	Met	Trp	Cys
Drosophila melanogaster	Leu	Ser	Ala	Glu	Gly	Val	Lys	Thr	Arg	Pro	Asp	Gln	Ile	Asn	Phe	Tyr	His	Met	Cys	Trp
Caenorhabditis elegans	Leu	Ser	Glu	Lys	Ala	Val	Ile	Thr	Gly	Arg	Asp	Asn	Phe	Pro	Gln	Tyr	Met	His	Cys	Trp
Leishmania major	Ala	Leu	Ser	Arg	Val	Gly	Thr	Pro	Glu	Asp	Gln	Lys	Ile	His	Phe	Asn	Tyr	Met	Cys	Trp
Sacch. cerevisiae	Leu	Ser	Lys	Ile	Glu	Asn	Thr	Asp	Val	Ala	Gly	Arg	Phe	Pro	Gln	Tyr	His	Met	Cys	Trp
Schizosacch. pombe	Leu	Ser	Glu	Lys	Ala	Ile	Val	Thr	Asp	Asn	Gly	Arg	Pro	Phe	Gln	Tyr	His	Met	Cys	Trp
Escherichia coli	Leu	Ala	Gly	Val	Ser	Ile	Glu	Thr	Arg	Asp	Lys	Gln	Pro	Asn	Phe	Tyr	Met	His	Trp	Cys
Bacillus subtilis	Leu	Ala	Ile	Glu	Lys	Gly	Val	Ser	Thr	Asp	Phe	Arg	Asn	Gln	Pro	Tyr	Met	His	Trp	Cys
Pseudom. aeruginosa	Leu	Ala	Gly	Arg	Val	Glu	Ser	Asp	Pro	Gln	Thr	Ile	Phe	Lys	Asn	Tyr	His	Met	Trp	Cys
Mesorhizobium loti	Ala	Leu	Gly	Val	Arg	Ser	Asp	Ile	Glu	Thr	Pro	Phe	Lys	Gln	Asn	Met	Tyr	His	Trp	Cys
Streptom. coelicolor A3	Ala	Leu	Gly	Val	Arg	Pro	Thr	Asp	Glu	Ser	Ile	Phe	Gln	His	Lys	Tyr	Asn	Met	Trp	Cys
Sinorhizobium meliloti	Ala	Leu	Gly	Val	Arg	Glu	Ser	Ile	Asp	Thr	Pro	Phe	Lys	Gln	Asn	Met	Tyr	His	Trp	Cys
Nostoc sp. PCC 7120	Leu	Ala	Ile	Val	Gly	Ser	Glu	Thr	Gln	Arg	Lys	Asp	Pro	Asn	Phe	Tyr	His	Met	Trp	Cys
Agrobact. tumefaciens	Ala	Leu	Gly	Val	Arg	Ser	Glu	Ile	Asp	Thr	Pro	Phe	Lys	Gln	Asn	Met	Tyr	His	Trp	Cys
Ralstonia solanacearum	Ala	Leu	Gly	Val	Arg	Thr	Asp	Pro	Ser	Glu	Ile	Gln	Phe	Lys	Asn	Tyr	His	Met	Trp	Cys
Yersinia pestis	Leu	Ala	Gly	Val	Ser	Ile	Glu	Thr	Arg	Asp	Gln	Lys	Pro	Asn	Phe	Tyr	Met	His	Trp	Cys
Methanosarc. acetivorans	Leu	Glu	Ile	Gly	Ser	Ala	Val	Lys	Thr	Asp	Arg	Asn	Phe	Pro	Tyr	Gln	Met	His	Cys	Trp
Vibrio cholerae	Leu	Ala	Val	Gly	Ser	Ile	Glu	Thr	Asp	Gln	Lys	Arg	Phe	Asn	Pro	Tyr	Met	His	Trp	Cys
Escherichia coli K12	Leu	Ala	Gly	Val	Ile	Ser	Glu	Arg	Thr	Asp	Gln	Pro	Lys	Asn	Phe	Tyr	Met	His	Trp	Cys
Mycobact. tuber. CDC1551	Ala	Leu	Gly	Val	Arg	Thr	Pro	Asp	Ser	Glu	Ile	Gln	Phe	Asn	His	Tyr	Lys	Met	Trp	Cys
Mycobact. tuber. H37Rv	Ala	Gly	Leu	Val	Arg	Thr	Asp	Pro	Ser	Glu	Ile	Gln	Phe	Asn	His	Tyr	Lys	Met	Trp	Cys
Bacillus halodurans	Leu	Glu	Val	Ala	Gly	Ile	Lys	Ser	Thr	Asp	Arg	Phe	Gln	Pro	Asn	Tyr	Met	His	Trp	Cys
Clostridium acetobutylicum	Ile	Lys	Leu	Ser	Glu	Val	Asn	Gly	Ala	Asp	Thr	Phe	Tyr	Arg	Pro	Met	Gln	His	Cys	Trp
Caulobacter crescentus CB15	Ala	Leu	Gly	Val	Arg	Asp	Pro	Glu	Thr	Ser	Ile	Phe	Lys	Gln	Asn	Met	Tyr	His	Trp	Cys
Synechocystis sp. PCC 6803	Leu	Ala	Gly	Val	Ile	Glu	Ser	Gln	Thr	Pro	Arg	Asp	Lys	Asn	Phe	Tyr	Met	His	Trp	Cys
Sulfolobus solfataricus	Leu	Ile	Lys	Val	Glu	Ser	Gly	Ala	Asn	Tyr	Arg	Thr	Asp	Phe	Pro	Gln	Met	His	Trp	Cys
Mycobacterium leprae	Ala	Leu	Val	Gly	Arg	Thr	Ser	Asp	Pro	Glu	Ile	Gln	Phe	Lys	Asn	His	Tyr	Met	Trp	Cys
Brucella melitensis	Ala	Leu	Gly	Val	Arg	Ile	Glu	Ser	Asp	Thr	Pro	Lys	Phe	Gln	Asn	Met	Tyr	His	Trp	Cys
Deinococcus radiodurans	Ala	Leu	Gly	Val	Arg	Pro	Thr	Glu	Ser	Asp	Gln	Ile	Phe	Lys	Asn	Tyr	His	Met	Trp	Cys
Listeria monocytogenes	Leu	Ile	Ala	Glu	Lys	Val	Gly	Thr	Ser	Asp	Asn	Phe	Arg	Pro	Gln	Tyr	Met	His	Trp	Cys
Clostridium perfringens	Ile	Leu	Lys	Glu	Gly	Val	Asn	Ser	Asp	Ala	Thr	Phe	Tyr	Arg	Pro	Met	Gln	His	Cys	Trp

